A G^1 AND A G^2 SUBDIVISION SCHEME FOR TRIANGULAR NETS*

HARTMUT PRAUTZSCH and GEORG UMLAUF

Fakultät für Informatik, Universität Karlsruhe
D-76128 Karlsruhe, Germany
E-mail: [prau/umlauf]@ira.uka.de

In this article we improve the butterfly and Loop's algorithm. As a result we obtain subdivision algorithms for triangular nets which can be used to generate G^1- and G^2-surfaces, respectively.

Keywords: Subdivision, interpolatory subdivision, Loop's algorithm, butterfly algorithm.

1. Introduction

Subdivision algorithms are popular in CAGD since they provide simple, efficient tools to generate arbitrary free form surfaces. For example, the algorithms by Catmull and Clark [1] and Loop [2] are generalizations of well-known spline subdivision schemes. Therefore the surfaces produced by these algorithms are piecewise polynomial and at ordinary points curvature continuous.

At extraordinary points however, the curvature is zero or infinite. In general, singularities at extraordinary points is an inherent phenomenon of subdivision, see [3, 4, 5].

The smoothness of a subdivision surface at its extraordinary points depends on the spectral properties of the associated subdivision matrix.

Doo and Sabin [6] derived necessary conditions on the eigenvalues. Ball and Storry [7, 8] made first rigorous investigations to prove the tangent plane continuity for a class of Catmull/Clark type algorithms. Then Reif [9] observed that tangent plane continuous surfaces may have local self-intersections and introduced the characteristic map defined by the subdominant eigenvectors. Moreover, for all stationary subdivision schemes he derived necessary and sufficient conditions which guarantee that the limiting surface is regular, i.e. tangent plane continuous without local penetrations.

*Supported by IWRMM and DFG grant # PR 565/1-1.

Finally, in [10] Reif's characteristic map is used to parametrize the subdivision surface. With this parametrization it is possible to extent Reif's result and to obtain for all stationary subdivision schemes necessary and sufficient conditions which guarantee that the limiting surface is a regular G^k-surface.

Doo and Sabin [6], Ball and Storry [8] and Loop [2] used the smoothness criteria to find among certain variations of the Catmull/Clark and Loop's algorithm the best. However, these best algorithms still produce curvature discontinuous surfaces, see e.g. [8].

In [11] we took a different approach. Instead of varying the subdivision rules within some bounds which are set heuristically, we changed the spectrum of the subdivision matrix so as to obtain the desired properties. Using the G^2-characterization in [10] we derived a G^2-subdivision algorithm from the Catmull/Clark algorithm (which does not produce infinite curvatures), see [11].

Here we provide similar improvements, a G^1- and a G^2-algorithm based on the butterfly and Loop's algorithm.

2. Loop's algorithm

Loop's algorithm generalizes the subdivision algorithm for surfaces expressed in terms of the symmetric quartic box spline over a regular triangulation of $\mathbb{R}^2$. It generates from any triangular net $\mathcal{N}_0$ a new net $\mathcal{N}_1$, whose vertices are classified as E- and V-vertices.

Computing the weighted averages of the four vertices of any two triangles in $\mathcal{N}_0$ sharing a common edge with the weights shown in Figure 1 gives the E-vertices. Similarly computing the weighted averages of all vertices of all triangles in $\mathcal{N}_0$ around any vertex with the weights shown in Figure 1 gives the V-vertices. For $n = 6$ Loop chooses $\alpha = 5/8$ since this corresponds to box spline subdivision.

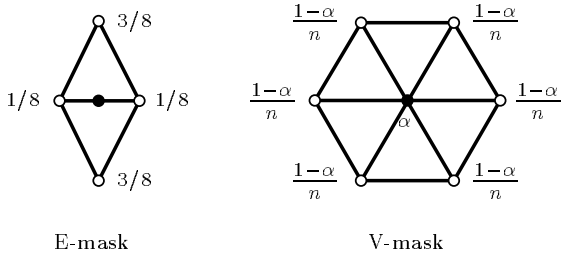

Fig. 1. The masks of the Loop algorithm – the V-mask is illustrated for $n = 6$.

The new net $\mathcal{N}_1$ is obtained by connecting for all triangles of $\mathcal{N}_0$ the associated three E-vertices and for all edges of $\mathcal{N}_0$ the associated E-vertices with both associated V-vertices. By the same procedure a next net $\mathcal{N}_2$ is obtained from $\mathcal{N}_1$ and so on.

A vertex of any net $\mathcal{N}_i, i \geq 1$, is called *extraordinary*, if it is an interior vertex with valence $\neq 6$. An extraordinary vertex of $\mathcal{N}_i$ is a V-vertex associated with an extraordinary vertex of $\mathcal{N}_{i-1}$. Thus the number of extraordinary vertices is constant for all nets $\mathcal{N}_i, i \geq 0$, and these vertices are separated by more and more ordinary vertices as i grows.

In particular if $\mathcal{N}_0$ is a regular triangular net, i.e. without extraordinary vertices, Loop's algorithm coincides with the subdivision algorithm for quartic box spline surfaces. Thus also for an arbitrary net $\mathcal{N}_0$ the sequence $\mathcal{N}_i$ converges to a piecewise quartic surface with one extraordinary point for each extraordinary vertex of $\mathcal{N}_0$. The limiting surface is a C^2-surface everywhere except at its extraordinary points.

Loop's analysis shows that the limiting surface has a continuous tangent plane at its extraordinary points for a certain range of α's, see [2] .

3. The butterfly algorithm

The butterfly algorithm of Dyn et al. [12] generates a sequence of triangular nets $\mathcal{N}_i, i \geq 0$, similar to Loop's algorithm. Only the masks used to compute the E- and V-vertices are different. They are given in Figure 2.

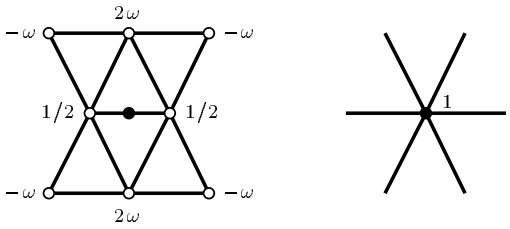

Fig. 2. The masks of the butterfly algorithm.

A sequence of nets $\mathcal{N}_i$ obtained by the butterfly algorithm with small positive ω converges to a surface that is differentiable everywhere except at its extraordinary points of valence 3 [12, 13] and $n \geq 8$.

At extraordinary points of valence $n \geq 8$ the surface is tangent plane continuous but it has self-intersections and therefore is not regular. We checked this for several ω. However, in the sequel we always work with $\omega = 1/32$.

Variations of the butterfly algorithm have been proposed by Zorin et al. [14]. Recently these variations were proved to generate regular G^1-surfaces [15].

4. A smoothness condition

In Sections 5 and 6 we present modifications of Loop's and the butterfly algo-

rithm giving G^2- or G^1-surfaces in the limit. The method used to derive these modifications is based on the G^k-analysis of subdivision schemes given in [10] and can also be used for subdivision schemes for quadrilateral nets [11].

For more details we need to recall a result from [10]. We present it in the theorem below for any *subdivision scheme* $\mathcal{S}$ that is identical with the butterfly or Loop's algorithm except that E- and V-masks may be different.

We assume that the limiting surface associated with any initial triangular net $\mathcal{N}_0$ obtained by the subdivision scheme $\mathcal{S}$ has C^k-parametrizations around all its ordinary points.

Extraordinary points are isolated as observed in Section 2. Therefore, to analyze the smoothness of the limiting surface at extraordinary points it suffices to consider a subnet $\mathcal{M}_0$ of $\mathcal{N}_0$ consisting of one extraordinary vertex surrounded by say r_0 rings of ordinary vertices as illustrated in Figure 3 for $r_0 = 3$.

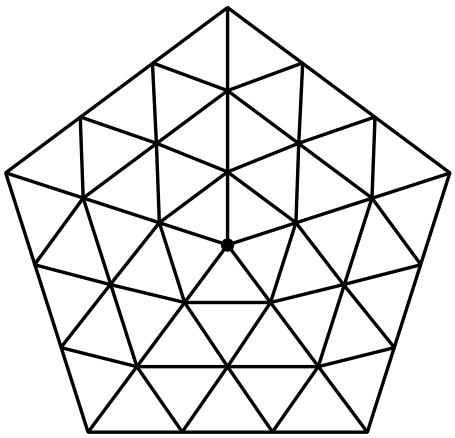

Fig. 3. A net with one extraordinary vertex of valence 5 (marked by •) surrounded by $r_0 = 3$ rings of ordinary vertices.

Further let $\mathcal{M}_1$ be the largest subnet of $\mathcal{N}_1$ whose vertices depend only on $\mathcal{M}_0$. This net $\mathcal{M}_1$ also has only one extraordinary vertex surrounded by say r_1 rings of ordinary vertices and in case of the butterfly algorithm by a further incomplete ring of V-vertices. To make $\mathcal{M}_1$ of a similar form as $\mathcal{M}_0$ we delete such an incomplete ring which modifies the definition of $\mathcal{M}_1$.

Note that r_1 is roughly twice as lage as r_0. For example in Loop's algorithm $r_1 = 5$ if $r_0 = 3$ and in the butterfly algorithm $r_1 = 6$ if $r_0 = 4$.

Let r_0 be so large that $r_1 - r_0 \geq 1$. Then discarding the $r_1 - r_0$ outer rings of $\mathcal{M}_1$ gives a net $\mathcal{K}_1$ with the same size and connectedness as $\mathcal{M}_0$. Let $\mathbf{m}_1, \ldots, \mathbf{m}_m$ and $\mathbf{k}_1, \ldots, \mathbf{k}_m$ denote the vertices of $\mathcal{M}_0$ and $\mathcal{K}_1$, respectively. Since the vertices $\mathbf{k}_i$ are affine combinations of the $\mathbf{m}_j$, there is an $m \times m$

matrix A such that

$$[\mathbf{k}_1 \ \dots \ \mathbf{k}_m]^t = A[\mathbf{m}_1 \ \dots \ \mathbf{m}_m]^t.$$

Let $\mathbf{s}_0$ denote the limiting surface associated with $\mathcal{M}_0$ under the subdivision scheme $\mathcal{S}$. Applying $\mathcal{S}$ to $\mathcal{M}_1$ gives the same limiting surface $\mathbf{s}_0$, but the surface $\mathbf{s}_1$ associated with the subnet $\mathcal{K}_1$ is smaller and only a part of $\mathbf{s}_0$. Taking $\mathbf{s}_1$ away from $\mathbf{s}_0$ gives the here so-called *first surface ring associated with* $\mathcal{M}_0$.

Now we are able to present the following theorem which is proven in a more general form in [10] :

Theorem 1 *Let A have the m (possibly complex) eigenvalues $1, \lambda, \lambda, \mu, \dots, \zeta$, where $1 > |\lambda| \geq |\mu| \geq \cdots \geq |\zeta|$ and assume two eigenvectors $\mathbf{c}$ and $\mathbf{d}$ associated with the double for simplicity real eigenvalue λ. If the first surface ring of the net given by $[\mathbf{c}_1 \dots \mathbf{c}_m]^t = [\mathbf{c}\,\mathbf{d}]$ is regular without self-intersections and*

$$|\lambda|^k > |\mu|, \quad k \geq 1, \tag{1}$$

then the limiting surface is a G^k-surface for almost all initial nets $\mathcal{M}_0$.

Remark 2 *More precisely, if Theorem 1 is satisfied, the limiting surface is a G^k-surface for all initial nets $\mathcal{M}_0$ whose expansion by the eigenvectors of A involves $\mathbf{c}$ in one and $\mathbf{d}$ in a second coordinate.*

The eigenvalue condition (1) goes back to Doo and Sabin [6]. The first surface ring associated with the eigenvectors $\mathbf{c}$ and $\mathbf{d}$ is called the *characteristic map of A* by Reif who used it to prove this Theorem for $k = 1$ [9]. An example for the characteristic map of Loop's algorithm is shown in Figure 4.

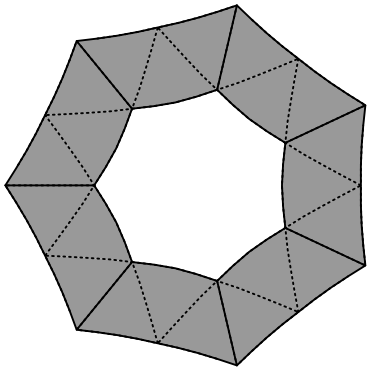

Fig. 4. The characteristic map of Loop's algorithm at an extraordinary vertex of valence $n = 7$.

If the limiting surface in Theorem 1 is a C^k-manifold, $k \geq 2$, then the extraordinary point is a flat point. This fact is also true for more general subdivision schemes, see [4, 5].

5. Modifications of Loop's algorithm

The subdivision matrix A of Loop's algorithm associated with an extraordinary vertex of valence n has a single dominant eigenvalue 1 and satisfies the G^1-conditions of Theorem 1 [2, 16], but not the G^2-condition [17]. To obtain a subdivision matrix A' that represents a modification of Loop's algorithm satisfying the G^2-condition we diagonalize the matrix A,

$$A = V\Lambda V^{-1}, \qquad \text{where } \Lambda = \operatorname{diag}(1, \lambda, \lambda, \mu, \ldots, \zeta),$$

change the modal matrix Λ to

$$\Lambda' = \Lambda + \operatorname{diag}(0, 0, 0, \delta_\mu, \ldots, \delta_\zeta), \qquad \text{where } |\mu + \delta_\mu|, \ldots, |\zeta + \delta_\zeta| < \lambda^2,$$

and compute the new subdivision matrix as

$$A' = V\Lambda' V^{-1}. \tag{2}$$

Lemma 3 *The matrices A and A' have the same characteristic maps.*

Proof The eigenvectors associated with λ are the same for A and A'. They define a planar control net $\mathcal{N}_0$. Subdividing $\mathcal{N}_0$ by Loop's algorithm and also by the modification results both times in the same sequence of nets $\mathcal{N}_i$. The extraordinary vertex and its three surrounding rings of control points in $\mathcal{N}_i$ are scaled versions of $\mathcal{N}_0$. The other control points of $\mathcal{N}_i$ are computed by the subdivision rules for regular nets. Thus Loop's algorithm and its modification applied to $\mathcal{N}_0$ produce the same surface in the limit. □

The symmetry of Loop's scheme means that the subdivision matrix A is block-circulant. Therefore a discrete Fourier transformation can be used to analyze the spectral properties of A.

If $n = 3$, the matrix A has the subdominant eigenvalue $\lambda = 1/4$ and exactly six eigenvalues with modulus in the half-open interval $[|\lambda|^2, |\lambda|)$. These are the two triple eigenvalues $1/8$ and $1/16$. Changing just these triple eigenvalues to the triple eigenvalues $1/8 + \varepsilon_1$ and $1/16 + \varepsilon_2$, respectively, such that $|1/8 + \varepsilon_1|$ and $|1/16 + \varepsilon_2|$ are less than $|\lambda|^2$, results in a matrix A', which represents the same masks as the original matrix A except for the E- and V-masks shown in Figure 5, where

$$\begin{aligned}
\beta_0 &= \frac{1}{8} + \frac{\varepsilon_1}{2(2\alpha - 1)}, & \gamma_0 &= \frac{1}{16} + \frac{\varepsilon_1}{2\alpha - 1} - \frac{3\varepsilon_2}{16\alpha - 7},\\
\beta_1 &= \frac{3}{8} - \frac{(16\alpha - 7)\varepsilon_1}{6(2\alpha - 1)}, & \gamma_1 &= \frac{5}{8} - \frac{(16\alpha - 7)\varepsilon_1}{3(2\alpha - 1)} - \frac{(16\alpha - 10)\varepsilon_2}{3(16\alpha - 7)},\\
\beta_2 &= \frac{1}{8} + \varepsilon_1, & \gamma_2 &= \frac{1}{16} + \varepsilon_2,\\
\beta_3 &= \frac{(20\alpha - 11)\varepsilon_1}{6(2\alpha - 1)}, & \gamma_3 &= \frac{1}{16} + \varepsilon_1 - \varepsilon_2,\\
& & \gamma_4 &= \frac{1}{16} + \frac{(2\alpha - 2)\varepsilon_1}{3(2\alpha - 1)} + \frac{(32\alpha - 11)\varepsilon_2}{3(16\alpha - 7)}.
\end{aligned}$$

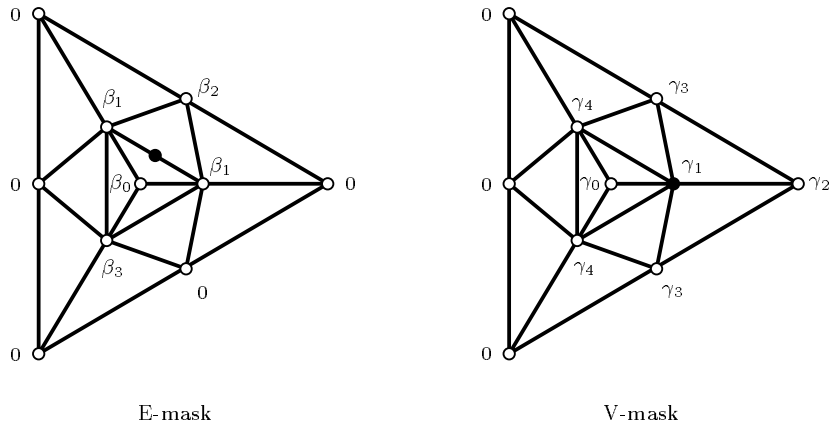

Fig. 5. The E- and V-masks of the modified Loop algorithm near a vertex of valence $n = 3$.

If $n \geq 4$, the matrix A has $k := \lfloor (n-1)/2 \rfloor - 1$ double eigenvalues besides λ. We denote these eigenvalues by $\mu_1, \ldots, \mu_k$ and assume $|\mu_1| \geq \cdots \geq |\mu_k|$. Furthermore, any eigenvalue of A with modulus in the half-open interval $[|\lambda|^2, |\lambda|)$ is one of these double eigenvalues μ_i but not vice versa.

Changing just these double eigenvalues μ_i to the double eigenvalues $\mu_i + \delta_i$ results in a matrix A', which represents the same masks as the original matrix except for the E-mask illustrated in Figure 6, where

$$\alpha_i = f_i + \frac{2}{n} \sum_{j=1}^{k} \delta_j \cos\left(\frac{2\pi i(j+1)}{n}\right), \; i = 0, \ldots, \lfloor n/2 \rfloor$$

and

$$f_i = \begin{cases} 3/8 & \\ 1/8 & \text{if } \; i = 1 \\ 0 & \end{cases} \begin{matrix} \\ \\ i \geq 2 \end{matrix} .$$

Note that Loop's masks, see Figure 1, are obtained if all δ's and ε's are zero.

Figure 7 shows an example. The left surface is generated using Loop's algorithm while the right one is produced with the above modified masks, where $\delta_1 = 0.03755$ and $\delta_2 = \cdots = \delta_k = 0$. The surfaces are shown with the visualization of their Gaussian curvature. To compute the curvature we iterated the algorithm until the hole became smaller than one pixel and then used the piecewise quartic parametrization of the surface and not a discrete approximation based on the subdivided control net. The common control net of both surfaces is given in Figure 8.

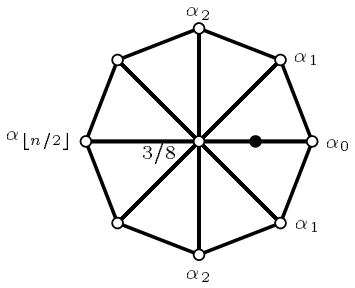

E-mask

Fig. 6. The E-masks of the modified Loop algorithm near the vertices of valence $n \geq 4$ illustrated for $n = 8$.

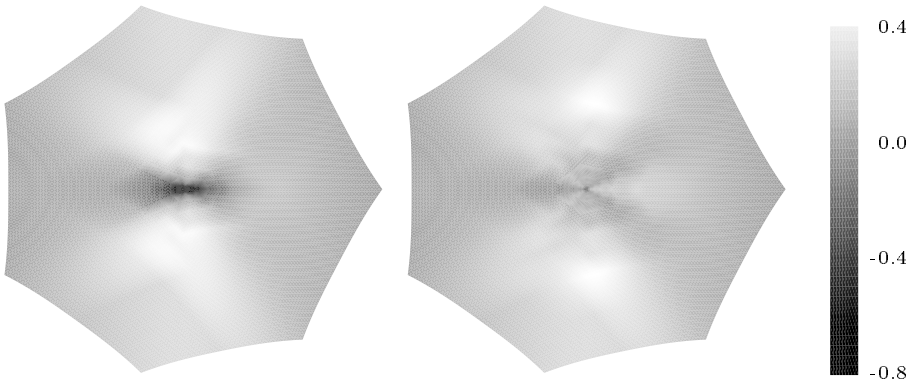

Fig. 7. Visualization of the Gaussian curvature of the surface generated from the net shown in Figure 8 by Loop's algorithm (left) and our modification (right).

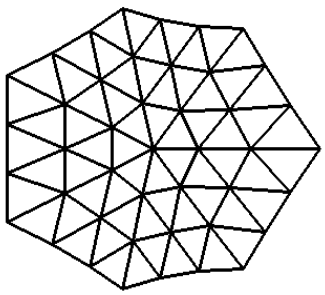

Fig. 8. Topview of the control net used for Figure 7. It lies on a parabolic cylinder.

Remark 4 *In some cases better looking surfaces are obtained if Loop's algorithm is gradually modified after each subdivision iteration. For example, starting from the net $\mathcal{N}_0$ shown in Figure 10 the sequence of nets $\mathcal{N}_i, i = 0, \ldots, 6$, leading to the surface shown in Figure 9 (bottom left) has been obtained by Loop's algorithm modified with $\varepsilon_1 = 2\varepsilon_2 = \sqrt{i/384}$ when applied to the net $\mathcal{N}_i$. In further iterations we would chose ε_1 and ε_2 constant as in step 6. Note that the modified subdivision matrix satisfies the conditions of Theorem 1 for $i \geq 2$.*

The adaptive linear combination of Loop's and our scheme produces a surface with a more even curvature distribution and without infinite curvature.

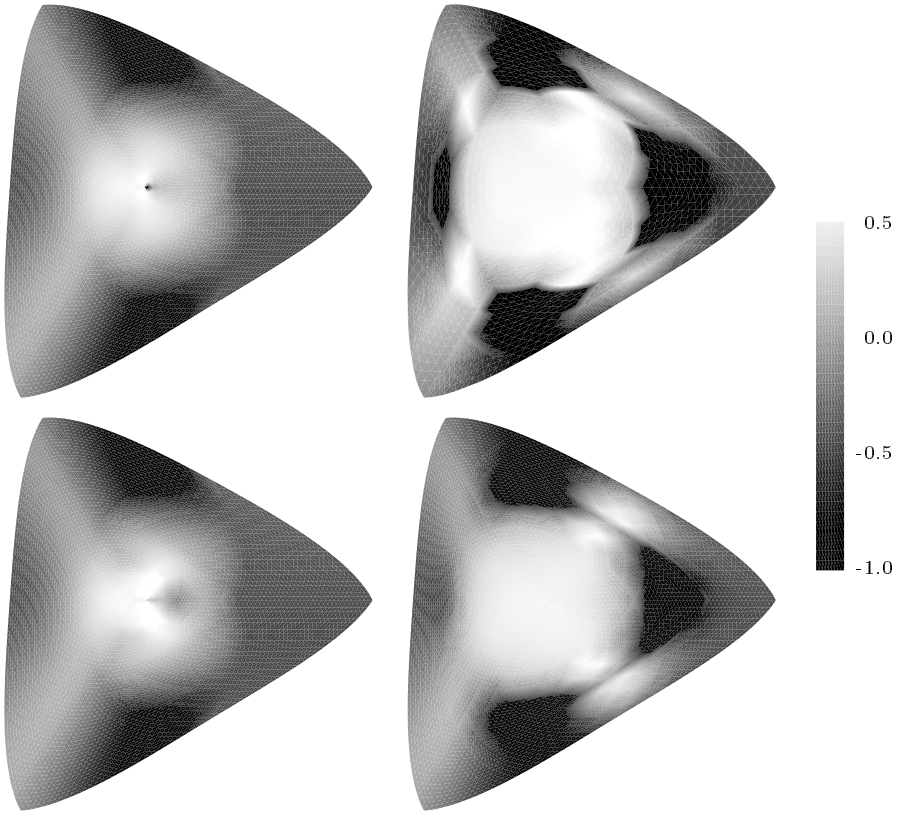

Fig. 9. Visualization of the Gaussian curvature of the surface generated from the net shown in Figure 10 by Loop's algorithm (top left), our modified scheme (top right), an adaptive linear combination of Loop's and our scheme (bottom left) and our modified scheme using the thin plates energy to determine the weights of the masks (bottom right).

Remark 5 *The eigenvalues of A with modulus less than $|\lambda|^2$ need not be changed. However, the masks of the modified algorithms depend linearly on $\delta_\mu, \ldots, \delta_\zeta$, see (2). Therefore quadratic energy functionals can be used to determine the optimal*

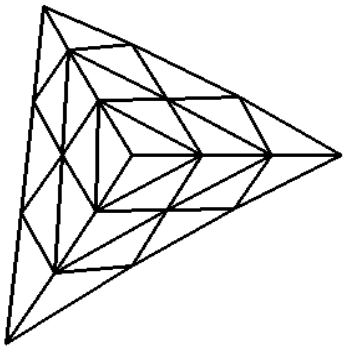

Fig. 10. Topview of the control net used for Figure 9. It lies on a hyperbolic paraboloid.

values for $\delta_\mu, \ldots, \delta_\zeta$.

An example surface is shown in Figure 9 (bottom right). Starting from the initial net of Figure 10 the surface is computed by the modified Loop algorithm using the thin plates energy to provide the weights for the masks.

6. Modifications of the butterfly algorithm

A limiting surface obtained by the butterfly algorithm is not differentiable at extraordinary points, in general. This can be seen from the associated subdivision matrix A which is block-circulant

$$A = \begin{bmatrix} A^0 & A^1 & \cdots & A^{n-1} \\ A^{n-1} & A^0 & \cdots & A^{n-2} \\ \vdots & & \ddots & \vdots \\ A^1 & \cdots & A^{n-1} & A^0 \end{bmatrix}.$$

Let $\widehat{A} = \mathrm{diag}(\widehat{A}^0, \ldots, \widehat{A}^{n-1})$ be the discrete Fourier transform of A. Then the blocks $\widehat{A}^i, i = 0, \ldots, n-1$, are given by

$$\widehat{A}^i = \left[\begin{array}{c|c|c|c} \delta_{i,0} & & & \\ \hline * & \widehat{L}^i & & \\ \hline * & * & \widehat{R}^i & \\ \hline * & * & * & O \end{array}\right],$$

with the Kronecker symbol $\delta_{i,0}$, the 4×4 zero-matrix O and

$$\widehat{L}^i = \begin{bmatrix} \frac{1}{2} + (4c_n^i - 2c_n^{2i})\omega & 0 & -(1 + a_n^{-i})\omega \\ 1 & 0 & 0 \\ \frac{1+a_n^i}{2} - (a_n^{-i} + a_n^{2i})\omega & -(1 + a_n^i)\omega & 2\omega \end{bmatrix},$$

$$\widehat{R}^i = \begin{bmatrix} 0 & -\omega & -a_n^{-i}\omega \\ 0 & -\omega & 0 \\ 0 & 0 & -\omega \end{bmatrix}$$

and $a_n = \exp(2\pi\sqrt{-1}/n), c_n^i = \mathrm{Re}(a_n^i)$. The eigenvalues of A are the eigenvalues of the blocks $\widehat{A}^i, i = 0, \ldots, n-1$, and are as follows:

- a simple eigenvalue 1,
- a $(6n-1)$-fold eigenvalue 0,
- a $2n$-fold eigenvalue $-\omega$ and
- the eigenvalues of $\widehat{L}^i, i = 0, \ldots, n-1$.

For an extraordinary vertex of valence 3, the largest eigenvalue of $\widehat{L}^0, \widehat{L}^1$ and $\widehat{L}^2$ is $(1 + \sqrt{1 - 16\omega})/4$. Therefore the subdominant eigenvalue λ is the triple eigenvalue $\lambda = (1 + \sqrt{1 - 16\omega})/4$ whose associated eigenvectors are linearly independent. So the limiting surface is not differentiable at an extraordinary point for valence 3.

However, the leading eigenvalues of $\widehat{L}^1$ and $\widehat{L}^2$ are associated with eigenvectors forming a regular and injective characteristic map. As in Section 5 we write $\widehat{L}^0$ as

$$\widehat{L}^0 = \widehat{V}_0 \Lambda \widehat{V}_0^{-1}, \quad \text{where } \Lambda = \mathrm{diag}(\lambda, \mu, 4\omega),$$

and (see [18])

$$\widehat{V}_0 = \begin{bmatrix} \lambda & \mu & 4\omega \\ 1 & 1 & 1 \\ \psi_\lambda & \psi_\mu & \psi_{4\omega} \end{bmatrix}, \qquad \psi_\nu = \frac{\nu(1 + 4\omega - 2\nu)}{4\omega}$$

where $\nu \in \{\lambda, \mu, 4\omega\}$. Changing the leading eigenvalue λ to $\lambda + \varepsilon$, such that $|\lambda + \varepsilon|$ is less than λ results in a new modal matrix Λ' and a modified block $\widehat{L}^0$. The inverse, discrete Fourier transform gives the modified matrix A'. It differs from the initial matrix A at those blocks that depend on $\widehat{L}^0$. These are the second diagonal blocks, L^i, of the blocks A^i. Their modifications are

$$\begin{bmatrix} \alpha_{3i+1} & \alpha_{3i+2} & \alpha_{3i+3} \\ \beta_{3i+1} & \beta_{3i+2} & \beta_{3i+3} \\ \gamma_{3i+1} & \gamma_{3i+2} & \gamma_{3i+3} \end{bmatrix} = L^i + \frac{1}{3}\widehat{V}_0 \cdot \mathrm{diag}(\varepsilon, 0, 0) \cdot \widehat{V}_0^{-1}, \qquad i = 0, 1, 2.$$

From this we read of the masks of the modified butterfly algorithm which are shown in Figure 11, where we used

$$\begin{bmatrix} \alpha_0 \\ \beta_0 \\ \gamma_0 \end{bmatrix} = \begin{bmatrix} 1 \\ 1 \\ 1 \end{bmatrix} - \sum_{j=1}^{9} \begin{bmatrix} \alpha_j \\ \beta_j \\ \gamma_j \end{bmatrix}.$$

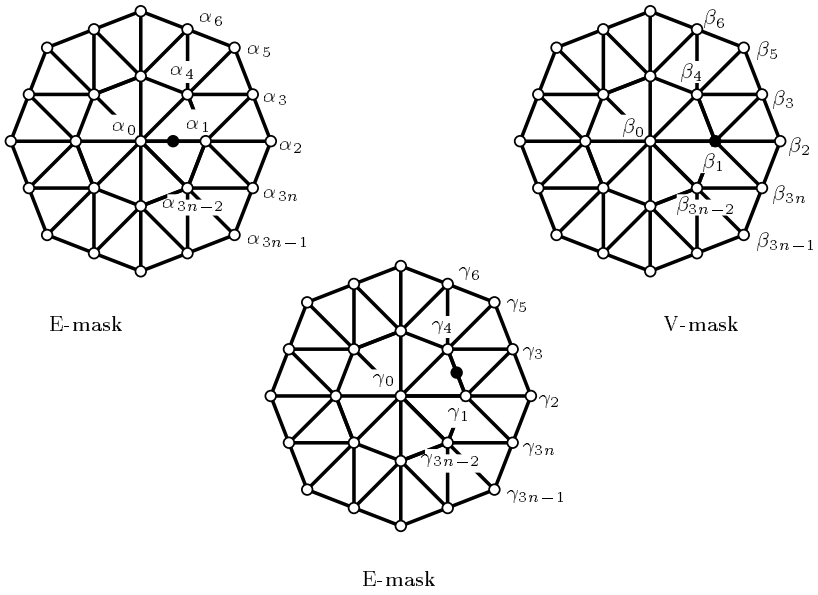

Fig. 11. The E- and V-masks of the modified butterfly algorithm near a vertex of valence $n = 8$.

For extraordinary vertices of valence $n = 4, \ldots, 7$ the limiting surface is a regular C^1-surface, see [19].

For an extraordinary vertex of valence $n \geq 8$ the subdominant eigenvalue λ comes from $\widehat{L}^i$ with $i \neq 1, n-1$. This means that the characteristic map of the subdivision matrix A overlaps itself, cf. [15, 20]. However, the largest eigenvalue of $\widehat{L}^1$ is associated with two eigenvectors representing the control net of a regular injective surface ring. So let λ_i denote the largest eigenvalue of $\widehat{L}^i, i = 1, \ldots, n-1,$. Then we change the eigenvalues $\lambda_i, i = 2, \ldots, n-2$, with modulus in $[|\lambda_1|, 1)$ to $|\lambda_i + \delta_i| < \lambda_1$ as in Section 5 so that λ_1 becomes the subdominant eigenvalue. The eigenvectors of $\widehat{L}^i, i = 2, \ldots, n-2$, form the matrices $\widehat{V}_i$ given by (see [18])

$$\widehat{V}_i = \begin{bmatrix} \lambda_i & \widetilde{\lambda}_i & \bar{\lambda}_i \\ 1 & 1 & 1 \\ \psi_{\lambda_i} & \psi_{\widetilde{\lambda}_i} & \psi_{\bar{\lambda}_i} \end{bmatrix}, \qquad \psi_\nu = \frac{\nu(1 + 4\omega(2c_n^i - c_n^{2i}) - 2\nu)}{4\omega c_n^{i/2}} a_n^{i/2}$$

for $\nu \in \{\lambda_i, \widetilde{\lambda}_i, \bar{\lambda}_i\} = \mathrm{spec}(\widehat{L}^i)$. This yields again the masks of Figure 11 with the weights

$$\begin{bmatrix} \alpha_{3i+1} & \alpha_{3i+2} & \alpha_{3i+3} \\ \beta_{3i+1} & \beta_{3i+2} & \beta_{3i+3} \\ \gamma_{3i+1} & \gamma_{3i+2} & \gamma_{3i+3} \end{bmatrix} = L^i + \frac{1}{n} \sum_{j=2}^{n-2} a_n^{ij} \widehat{V}_j \cdot \mathrm{diag}(\delta_j, 0, 0) \cdot \widehat{V}_j^{-1}$$

for $i = 0, \ldots, n-1$ and $\alpha_0 = 1/2, \beta_0 = 0, \gamma_0 = 2\omega$. Note that the weights are always real if $\delta_{\mu_i} = \delta_{\mu_{n-i}}$ for $i = 2, \ldots, \lfloor n/2 \rfloor$.

Figure 12 shows an example with an extraordinary vertex of valence $n = 14$. The top row shows the surfaces generated using the butterfly scheme (left) and the above modified masks (right) with the parameters $\omega = 1/20$ and $\delta_{\mu_i} = \mu_1 - \mu_i - 0.02$ for $\mu_i \geq \mu_1, i = 2, \ldots, n-2$. The bottom row shows a selective enlargement of some vicinity of the extraordinary point of the two surfaces, respectively. Note that the left surface has self-intersections while the right surface as well as the common control net of both surfaces, see Figure 13, have no self-intersections.

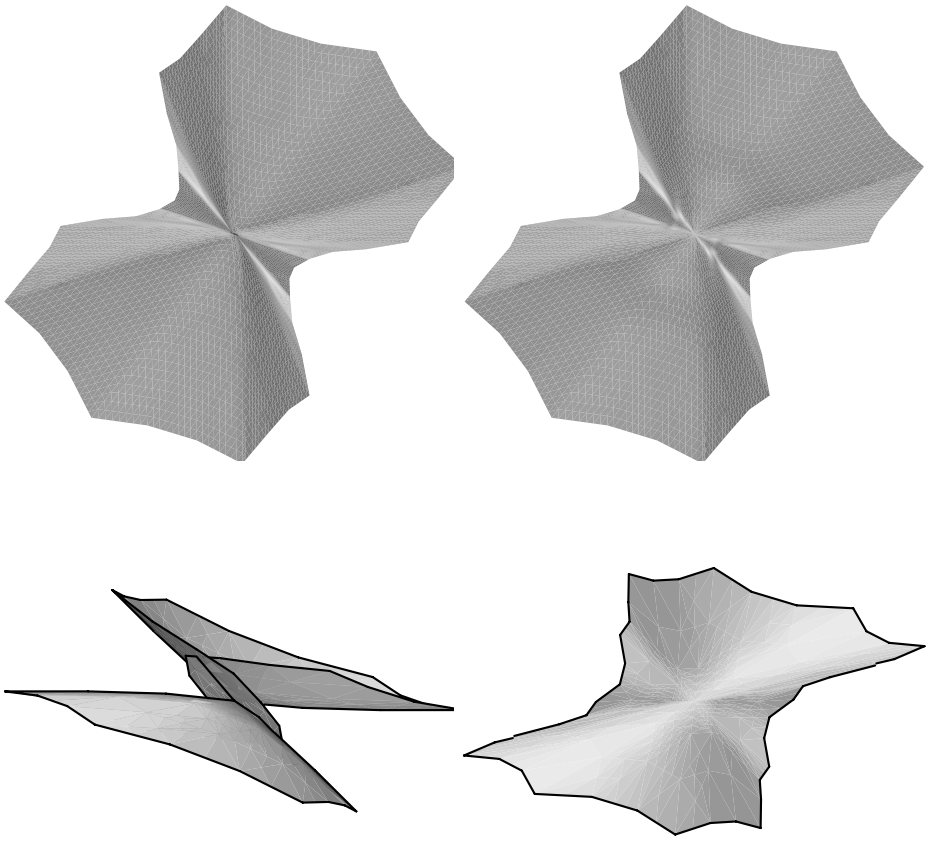

Fig. 12. The surface generated from the net shown in Figure 13 by the butterfly scheme (top left) and our modification (top right). The bottom row shows an enlargement of some vicinity around the extraordinary point of the two surfaces from a different perspective as the top row with their respective boundary curves.

Remark 6 *The surface obtained by the modified butterfly algorithm does not interpolate all vertices of the initial control net. However, if we use the butterfly*

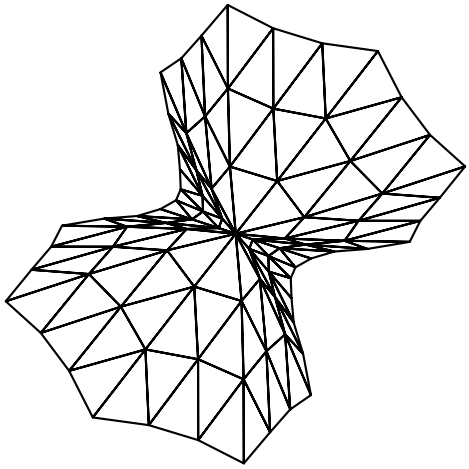

Fig. 13. The control net used for Figure 12.

algorithm in the first iteration and the modification in all further iterations, all vertices of the initial net are interpolated.

Acknowledgements

We wish to thank Keni Bernardin, Matthias John and Uwe Klotz who helped us to generate Figures 7, 9 and 12.

References

1. E. Catmull and J. Clark. Recursive generated b-spline surfaces on arbitrary topological meshes. *CAD*, 10(6):350–355, 1978.
2. C.T. Loop. Smooth Subdivision Surfaces Based on Triangles. Master's thesis, Department of Mathematics, University of Utah, August 1987.
3. M.A. Sabin. Cubic recursive division with bounded curvature. In P.J. Laurent, A. Le Méhauté, and L.L. Schumaker, editors, *Curves and Surfaces*, pages 411–414. Academic Press, Boston, 1991.
4. U. Reif. A degree estimate for subdivision surfaces of higher regularity. *Proceedings of the American Mathematical Society*, 124(7):2167–2174, 1996.
5. H. Prautzsch and U. Reif. Degree estimates for C^k-piecewise polynomial subdivision surfaces. *Computational Mathematics*, 10:209–217, 1999.
6. D.W.H. Doo and M. Sabin. Behaviour of recursive division surfaces near extraordinary points. *CAD*, 10(6):356–360, 1978.
7. A.A. Ball and D.J.T. Storry. A matrix approach to the analysis of recursively generated b-spline surfaces. *CAD*, 18(8):437–442, 1986.
8. A.A. Ball and D.J.T. Storry. Conditions for tangent plane continuity over recursiveley generated b-spline surfaces. *ACM Transactions on Graphics*, 7(2):83–102,

1988.

9. U. Reif. A unified approach to subdivision algorithms near extraordinary vertices. *CAGD*, 12:153–174, 1995.
10. H. Prautzsch. Smoothness of subdivision surfaces at extraordinary points. *Advances in Computational Mathematics*, 9:377–390, 1998.
11. H. Prautzsch and G. Umlauf. A G^2-subdivision algorithm. In G. Farin, H. Bieri, G. Brunnet, and T. DeRose, editors, *Geometric Modelling*, volume 13 of *Computing Suppl.*, pages 217–224. Springer-Verlag, 1998.
12. N. Dyn, J.D. Gregory, and D. Levin. A butterfly subdivision scheme for surface interpolation with tension control. *ACM Transactions on Graphics*, 9(2):160–169, 1990.
13. N. Dyn, D. Levin, and C.A. Micchelli. Using parameters to increase smoothness of curves and surfaces generated by subdivision. *CAGD*, 7:129–140, 1990.
14. D. Zorin, P. Schröder, and W. Sweldens. Interpolatory subdivision for meshes with arbitrary topology. *Computer Graphics (ACM SIGGRAPH '96 Proceedings)*, pages 189–192, 1996.
15. D. Zorin. *Stationary Subdivision and Multiresolution Surface Representations.* PhD thesis, California Institut of Technology, Pasadena, 1998.
16. G. Umlauf. Analyzing the characteristic map of triangular subdivision schemes. To appear: *Constructive Approximation*, 1999.
17. G. Umlauf. Verbesserung der Glattheitsordnung von Unterteilungsalgorithmen für Flächen beliebiger Topologie. Master's thesis, IBDS, Universität Karlsruhe, April 1996.
18. R. Shenkman, N. Dyn, and D. Levin. Normals of the butterfly subdivision scheme surfaces and their applications. *Journal of Computational and Applied Mathematics*, 102(1):157–180, 1999.
19. D. Zorin. A method for analysis of C^1-continuity of subdivision surfaces. Technical Report No. CLS-TR-98-764, Stanford University, 1998. Submitted to *SIAM Journal of Nmerical Analysis.*
20. J. Peters and U. Reif. Analysis of algorithms generalizing B-spline subdivision. *SIAM Journal on Numerical Analysis*, 35(2):728–748, 1998.